Chemical Physics Letters 501 (2011) 358–363

Contents lists available at ScienceDirect

Chemical Physics Letters

journal homepage: www.elsevier.com/locate/cplett

# Fluorescence dynamics in supercooled (acetamide + calcium nitrate) molten mixtures

Harun Al Rasid Gazi, Biswajit Guchhait, Snehasis Daschakraborty, Ranjit Biswas *

*S.N. Bose National Centre for Basic Sciences, JD Block, Sector III, Salt Lake, Kolkata 700 098, West Bengal, India*

ARTICLE INFO

*Article history:*
Received 28 October 2010
In final form 1 December 2010
Available online 3 December 2010

ABSTRACT

Fluorescence dynamics of a polar solute probe in molten ($CH_3CONH_2$ + $Ca(NO_3)_2{\cdot}4.37H_2O$) mixtures have been measured in order to probe the solute–medium interactions in such complex systems. Steady state and time-resolved measurements bear no signatures of mega-value of the static dielectric constant, strong heterogeneity and extremely slow relaxation times reported in dielectric relaxation experiments for these molten mixtures. Subsequent applications of a semi-molecular theory reveal both the solute–medium dipole–dipole and ion–dipole interactions contribute significantly to the measured Stokes' shifts. Calculated average solvation times in the underdamped and overdamped limits of frictional solvent response agree semi-quantitatively with those from time-resolved measurements.



## 1. Introduction

Acetamide, in its molten state (melting point ~353 K), can dissolve a large number of organic and inorganic compounds [1–4]. The ability of this amphoteric compound to both donate and accept proton coupled with its high dielectric constant ($\varepsilon_0 \approx 60$) [1,4] in molten state is responsible for its strong solvating power. Addition of certain electrolytes in acetamide leads to extensive freezing point depression, and as a result, binary or ternary mixtures of molten acetamide with inorganic salts have been extensively used for a variety of chemical and electrochemical applications [5–10]. Binary mixtures of acetamide and calcium nitrate tetrahydrate (m.p. ~316 K) form a liquid near room temperature even at 0.1 mol fraction of the alkaline earth salt and the glass transition temperature ($T_g$) of these mixtures is around 240 K [5,6]. Therefore, these molten binary mixtures near room temperature or a little above it are regarded as supercooled solutions where high viscosity and microscopic inhomogeneity characterize the systems [9]. Viscoelastic and ultrasonic relaxation experiments with molten mixtures at 0.24 mol fraction of calcium nitrate indicates aggregation of amide molecules in presence of the electrolyte [5]. Subsequent dielectric relaxation (DR) measurements indicate mega-value (~$10^6$) of the static dielectric constant ($\varepsilon_0$) for this mixture [7], and a more recent study of transport properties suggests the Vogel–Fulcher–Tammann (VFT) equation as an adequate descriptor for the measured temperature dependence for these quantities [9].

The reported very high value of $\varepsilon_0$ and the associated microscopic heterogeneity in these molten mixtures then naturally motivate one to investigate whether signatures of such solution characteristics can be reflected in the fluorescence spectroscopic experiments. Since the fluorescence spectral shift (relative to the gas phase) of a dissolved polar solute is governed by the local polarity and spectral width is affected by the local solution structure [11,12], steady state fluorescence spectroscopic experiments can indeed provide useful information regarding the solution polarity and heterogeneity. Time-resolved Stokes' shift experiments, on the other hand, generate time-profile of the dynamic response (or, in other words, solvation response) of these systems to an instantaneously created perturbation, careful analyses of which may reveal the presence or absence of solution heterogeneity [13]. Since the magnitude of dynamic Stokes' shift is determined by the solute–solvent interaction and solvation response time scale is a manifestation of the inherent pure solvent dynamics 'dressed' by the solute–solvent and solvent–solvent interactions [14–17], time-resolved fluorescence experiments can probe simultaneously the interactions and time-scales present in the system. Probing the solvation timescales via fluorescence experiments is particularly important because of its relationship to the frequency dependent dielectric function [18–20]. Curiously, available DR data [7,8] indicate extremely long relaxation time (millisecond to even a second) in the low frequency regime. A simple continuum model relation [18–20], $\tau_L \approx (\varepsilon_\infty/\varepsilon_0)\tau_D$, then predicts the existence of solvation timescale around a couple of hundred nanoseconds or even a few microseconds! Because of limited frequency range employed in these DR experiments, dispersions at higher frequency regime have also been completely missed and, therefore, a complete knowledge of the full dynamics of these molten mixtures is still lacking.

In this Letter, we have investigated the fluorescence dynamics by using a dipolar probe (coumarin 153, abbreviated as C153) in molten ($CH_3CONH_2$ + $Ca(NO_3)_2{\cdot}4.37H_2O$) binary mixtures at

* Corresponding author.
*E-mail address:* rbsnbc@gmail.com (R. Biswas).

0009-2614/$ - see front matter © 2010 Elsevier B.V. All rights reserved.
doi:10.1016/j.cplett.2010.12.003

$T \sim 318$ K with calcium salt mole fractions, $x_{salt}$ = 0.1, 0.25, 0.4 and 0.5. These mole fractions are chosen because there exist no macroscopic phase separation in these compositions at 318 K, and the molten mixtures are nicely into the liquid phase. The present study does not consider $x_{salt}$ higher than 0.5 because fluorescence quenching in mixtures at $x_{salt} > 0.5$ lowers the signal-to-noise ratio to an unacceptable level. Time-resolved fluorescence anisotropy measurements further explore the solute–medium interaction in these molten mixtures. Subsequently, a semi-molecular hydrodynamic theory [15] is employed to reveal the molecular origin of the timescales measured by the dynamic Stokes' shift experiments.

## 2. Experimental

Laser grade C153 (Exciton) and Formamide (FA, Sigma–Aldrich) were used as received. Acetamide ($\geqslant$99%, SRL, India) was vacuum dried (room temperature) over $P_2O_5$, Calcium nitrate ($\geqslant$99%, SRL, India) vacuum-dried overnight before use.

Steady state absorption (UV-2450, Shimadzu) and fluorescence (Fluoromax-3, Jobin–Yvon) spectra were collected and processed properly for further use. Time resolved fluorescence measurements were carried out using the time correlated single photon counting technique based on a laser system (LifeSpec-ps, Edinburgh Instruments) with 409 nm excitation light (band-pass of ±2 nm). The full width at half maximum of the instrument response function (*irf*) was ~70 ps. Method for sample preparation and details about the data collection and analyses of steady state and time-resolved spectra are already discussed in Ref. [15].

## 3. Results and discussion

### 3.1. Steady state spectroscopic studies

Representative steady state absorption and fluorescence emission spectra of C153 dissolved in a molten mixture at $x_{salt}$ = 0.4 are shown in Figure 1. In the same figure are shown the absorption and emission spectra of C153 in room temperature FA ($\varepsilon_0$ = 111) for comparison. Note the similarity in spectral positions and widths in these two different media. More quantitatively, the *average* absorption and emission spectral peak frequencies [21,22] for C153 in this mixture are respectively (in the unit of $10^3$ cm$^{-1}$) 22.91 and 17.55 which are comparable with those in FA (23.91 and 17.96). The spectral widths (full width at half maximum, fwhm) are also very similar in these media (in the unit of $10^3$ cm$^{-1}$): for absorption, 4.44 in melt versus 4.77 in FA and, for emission, 3.44 (melt) versus 3.44 (FA). The closeness in spectral properties with those in FA has also been found for other mixture compositions as well. This is demonstrated in Figure 2 where absorption and emission peak frequencies and the corresponding spectral widths are shown as a function of $x_{salt}$. This similarity is intriguing particularly when one compares the reported mega-value of the solution dielectric constant for these molten mixtures [5,7] with that of FA and the extent of heterogeneity present in melt. This comparison therefore indicates that the average polarity sensed by the solute in this molten mixture is not as huge as that reported in the existing DR study. In addition, the solution heterogeneity is not probably longer-lived (relative to the fluorescence life time of C153) to significantly affect the spectral width [23–26]. The mega-value of $\varepsilon_0$ for these molten mixtures, on the other hand, may arise from two sources: electrode polarization [27] and one-over-frequency ($1/\omega$) divergence in the measured over-all dielectric response of a conducting solution in the zero frequency limit [28]. It is then natural that the spectral positions are reflections of dipolar solute – dipolar solvent (dipole–dipole) and dipolar solute–ion (ion–dipole) interactions only.

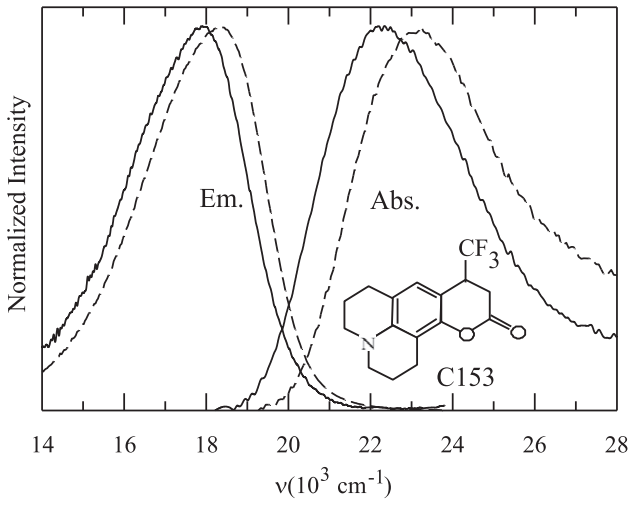


**Figure 1.** Steady state absorption and fluorescence emission spectra (solid line) of C153 dissolved in molten mixture at $x_{salt}$ = 0.4 at 318 K and in formamide (broken line) at room temperature. The chemical structure of C153 is also shown in the inset.

### 3.2. Time-resolved fluorescence spectroscopic studies

Typical fluorescence emission intensity decays collected at blue (470 nm) and red (660 nm) ends of the steady state emission spectrum of C153 dissolved in molten mixture at $x_{salt}$ = 0.25 are shown in Figure 3 along with the fitted curves and fit parameters. The corresponding residuals are also presented in the bottom panels which show the quality of these fits. Except the decays collected at wavelengths near the peak of the steady state emission spectrum which fit to bi-exponential functions, all other decays at this and other mixture compositions considered in this study require a

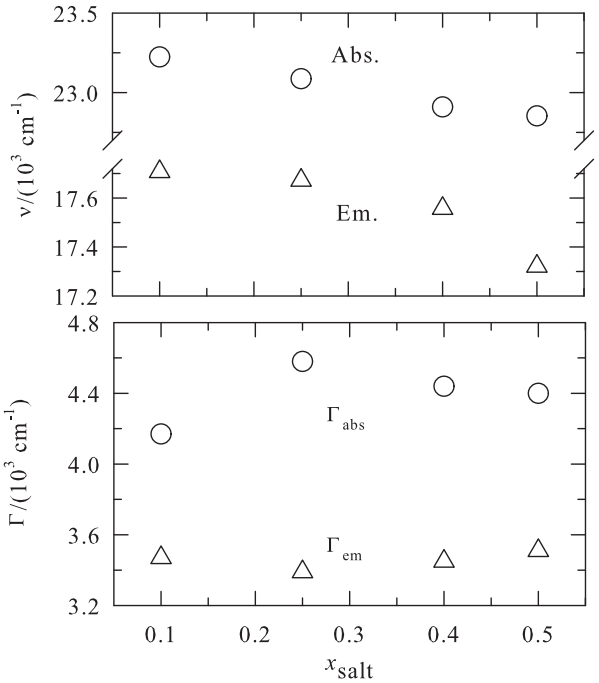


**Figure 2.** Salt concentration dependencies of absorption ('Abs') and emission ('Em') peak frequencies ($\nu$) are shown in the *upper panel* and those for full width at half maxima ($\Gamma$) are presented in the *lower panels*.

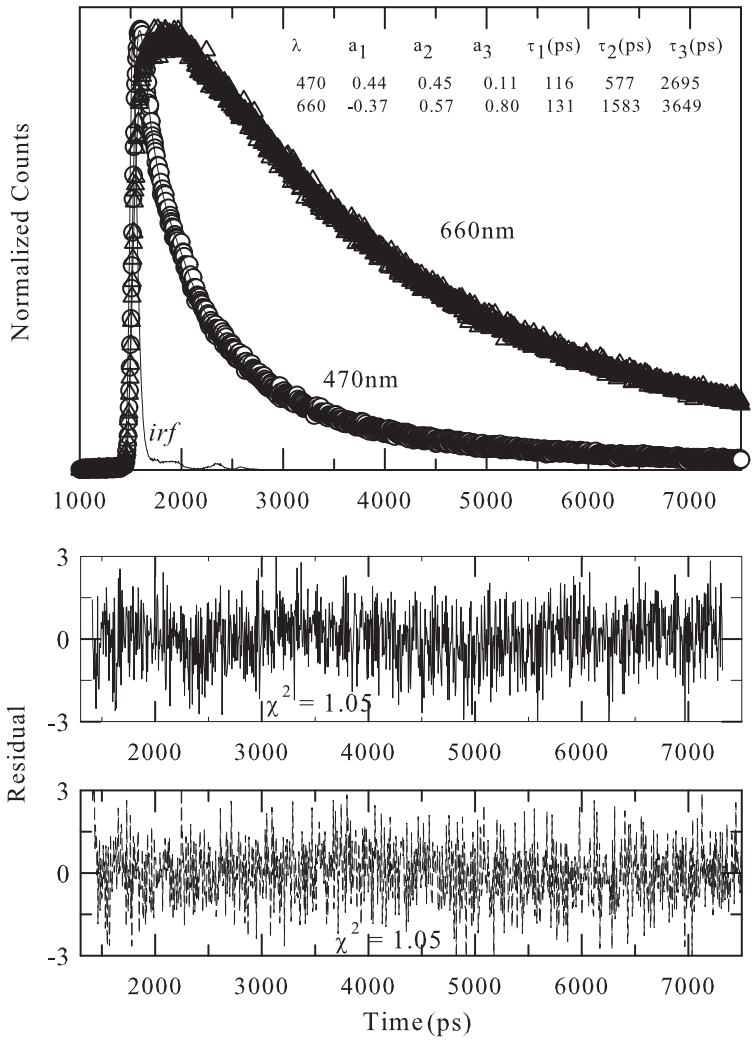


**Figure 3.** Representative fluorescence intensity decay of C153 at blue (470 nm) and red (660 nm) wavelengths at $x_{salt} = 0.25$ ($T \sim 318$ K). Experimental data are shown by circles (470 nm) and triangle (660 nm) while fit through them by solid lines. Instrument response function ('*irf*') represented by the solid line. The respective residuals – solid line (470 nm) and broken lines (660 nm) – are also presented. Inset shows the fit parameters and $\chi^2$ ('goodness-of-fit' parameter) values.

sum of three exponentials for adequate description. Note that while the decay at the shorter wavelength (blue-end) requires only decay components, the one at the longer wavelength (red-end) requires an additional rise component. Moreover, the time constants are also well-separated with significant amplitude associated with each of them. This suggests the presence of dynamic Stokes' shift in these molten mixtures. A concern is however whether dynamic fluorescence quenching also contributes to the measured decays. Our study of $x_{salt}$ dependence of the longest time constant has revealed change in values, on an average, ~6% at shorter wavelengths (blue-end) and ~20% at longer wavelengths across the mixture composition considered. The small change in the longest time constant indicates negligible contribution from the dynamic fluorescence quenching, and thus the dynamic Stokes' shift measured here originates – as commonly understood [11–20] – mainly from the rearrangement of the environment driven by a sudden alteration in the equilibrium electron distribution in a solute molecule via laser irradiation.

Time-resolved fluorescence emission spectra of C153 in melt mixture at $x_{salt} = 0.25$ are shown in Figure 4. The lines going through the symbols are obtained from fitting the reconstructed data points to a log-normal line shape function [11]. Note that the variation in width of these reconstructed time-resolved spectra is insignificant (within ±100 $cm^{-1}$) and this indicates that the spectrum moves physically in time as solvation progresses. Another aspect to notice in Figure 4 is that the steady state fluorescence spectrum at this salt concentration is nearly 200 $cm^{-1}$ 'blue-

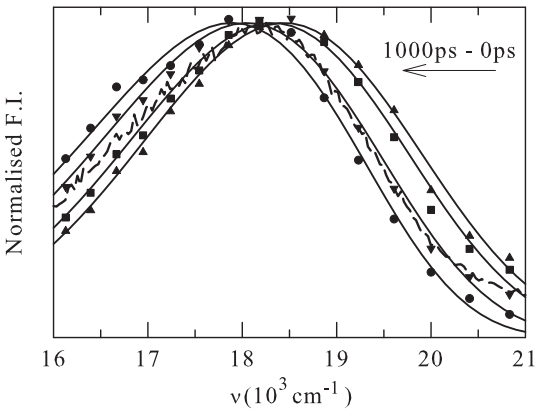


**Figure 4.** Synthesized time resolved emission spectra (TRES) of C153 at $x_{salt} = 0.25$ at four different time slices – 0 ps (triangles), 50 ps (squares), 250 ps (inverted triangles) and 1000 ps (circles). Steady state emission spectrum is shown by the broken lines.

shifted' compared to the time-resolved spectrum at $t = \infty$. As discussed earlier for molten mixtures of acetamide with sodium/potassium thiocyanates [15], this small difference between the steady state and $t = \infty$ spectra may originate either from a subtle modification in the vibronic structure of the spectrum or from the fluorescence emission (steady state) occurring from partially relaxed solvent configuration due to sluggish movement of solvent and/or ion–solvent composite species. The difference (peak to peak) between the reconstructed time-zero spectrum ($\nu(t = 0)$) and that at $t = \infty$ ($\nu(t = \infty)$) is ~850 $cm^{-1}$, which is ~40% less than the estimated 'true' dynamic Stokes' shift ($\Delta\nu^t_{est} \approx 1450\ cm^{-1}$) for C153 at this mixture composition. Estimation of 'true' dynamic Stokes' shift requires accurate determination of $\nu(t = 0)$ which has been obtained by following the approximation described in Ref. [29].

The magnitudes of true dynamic Stokes' shift so obtained at four different mixture compositions and the measured values are summarized in Table 1 where the undetected portions are also indicated. Data in this table indicate that the true value of the shift decreases as $x_{salt}$ increases and the detected shifts are approximately *half* of the true values at these compositions. Uniform missing of such a large fraction across the mixture composition suggests that these molten mixtures possess timescale which is much faster than the resolution employed [30]. The presence of an extremely fast timescale is expected in these mixtures as amide systems possess librational modes [31,32] and these collective intermolecular modes have been shown to produce ultrafast (<1 ps) response in dipolar solvation by H-bonded solvents [33–35]. Dynamic Stokes' shift measurements with C153 in alkyl amides have indeed shown the presence of a significant (~30–50%) sub-picosecond component in the total solvation response [11,29]. One then immediately asks what is the timescale of the missing component and wherefrom does it originate? What roles do the solute–solvent and solute–ion interactions play in determining the full dynamics? A molecular theory, developed earlier and applied to molten mixtures of acetamide with $Na^+/K^+$ thiocyanates [15], is used next to quantify the roles of solute–acetamide and solute–ion interactions and dynamics in these binary molten mixtures. However, before doing so, let us briefly discuss the possible reasons for the observed decrease in dynamic Stokes' shift upon increasing $x_{salt}$ in the melt.

Various relaxation studies [5,7] and measurements of transport properties with molten mixtures of acetamide with calcium nitrate [9] have suggested ion-induced aggregation of amide molecules. The extent of aggregation increases with the increase in ion concentrations in the mixture [9,10]. This probably reduces the number of free amide molecules to interact with the solute and thus the shift decreases. Note that at $x_{salt} = 0.1$ the estimated shift is ~1700 $cm^{-1}$ which compares well with the measured dynamic shift of about 1850 $cm^{-1}$ for C153 in FA and dimethylformamide (DMF, $\varepsilon_0$ 36.7) at ~298 K [11]. Aggregation in pure liquid formamide is well-known [33] and this solvent aggregation is probably responsible partially for similar Stokes' shifts (~1800–2200 $cm^{-1}$) measured [11] in solvents of very different $\varepsilon_0$ values, for example, FA, DMF, NMF ($\varepsilon_0 = 182.4$) and acetonitrile ($\varepsilon_0 = 35.94$). Interestingly, at $x_{salt} = 0.25$, the estimated shift in presence of calcium salt is ~1450 $cm^{-1}$ which is ~400 $cm^{-1}$ less than that in molten mixtures of acetamide with sodium thiocyanate (NaSCN) [15]. Dynamic Stokes' shift measurements with a coumarin derivative in 1.0 M electrolyte solutions of acetonitrile at ~296 K have also indicated much less shift in presence of $Ca^{+2}$ ions than that detected in presence of $Na^+$ ion [36]. All these observations probably suggest difference in solute–ion interactions due to variations in ion charge density.

The calculated values of the total dynamic Stokes shift for these molten mixtures and the separated dipole–dipole (solute–solvent) and ion–dipole (ion–solute) interaction contributions by using the theory described in Ref. [15] (also briefly in the supporting information) are provided in the last three columns of Table 1. Data in these columns indicate that the ion–dipole interaction contribution increases from ~30% to ~60% in changing $x_{salt}$ from 0.1 to 0.5 and, as a result, the total shift registers an over-all increase of ~45% in this salt concentration range. It is interesting to note that even-though these calculations predict a steady increase in total shift with $x_{salt}$, experimentally estimated shift has actually shown the reverse. The estimated shift at $x_{salt} = 0.5$ is, in fact, *half* of the calculated total value. This discrepancy between theory and experiment is mainly because of the salt being assumed to be fully dissociated in the theory whereas in real solutions a considerable fraction of salt remains as ion-pairs and other complex ionic species [37,38]. It is also known that concentration of free ions decreases but that of ion-pairs increases upon the increase of salt concentration in electrolyte solutions of polar solvents. This is probably the reason for the experimentally observed decrease of the true dynamic Stokes' shift with the increase in salt concentration in these molten mixtures. Note, however, that at $x_{salt} = 0.1$, where the complexity due to ion-pairing is expected to be relatively much less pronounced, the calculated shift (1490 $cm^{-1}$) agrees semi-quantitatively with the experimental estimate (1672 $cm^{-1}$).

Table 2 compares the experimental solvation timescales with those calculated by using the theory [15] discussed briefly in the supporting information. Experimental solvation response function, $S(t) = \frac{\nu(t)-\nu(\infty)}{\nu(0)-\nu(\infty)}$, obtained from the fitted time-resolved fluorescence emission spectra, has been found to be bi-exponential for all the four binary mixture compositions. The longer of these measured time constants ($\tau_2$) exhibit a clear viscosity dependence, indicating diffusive process as an origin for this timescale. However, the measured average solvation times, $\langle\tau_s\rangle = \int_0^\infty dtS(t)$, do not show such a clear viscosity dependence because of non-monotonic salt concentration dependence of the shorter time constant.

The origin of the experimental timescales is next investigated by using a semi-molecular hydrodynamic theory in the underdamped and overdamped limits of frictional solvent response [15–17]. The salient features and necessary expressions are provided in the supplementary information (Appendix 1). As shown earlier [16], calculations in the underdamped limit require experi-

**Table 1**
Dynamic Stokes' shift in molten ($CH_3CONH_2 + Ca(NO_3)_2{\cdot}4.37H_2O$) mixtures: comparison between theory and experiments.

| $x_{salt}$ | $T/K$ | $\eta$ (cP) | $\rho$ (g/cm3) | Experiment[a] | | | Theory[b] | | |
|---|---|---|---|---|---|---|---|---|---|
| | | | | True shift ($cm^{-1}$) | Shift observed ($cm^{-1}$) | % Missed | Dip–dip contribution $\Delta\nu^t_{sd}$ ($cm^{-1}$) | Ion–dip contribution $\Delta\nu^t_{si}$ ($cm^{-1}$) | Total shift ($cm^{-1}$) |
| 0.1 | 318 | 21.8 | 1.179 | 1672 | 756 | 54.78 | 1052 | 438 | 1490 |
| 0.25 | 318 | 31.7 | 1.314 | 1451 | 854 | 41.48 | 956 | 793 | 1749 |
| 0.4 | 318 | 41.6 | 1.432 | 1368 | 616 | 55.0 | 919 | 1086 | 2005 |
| 0.5 | 318 | 47.4 | 1.504 | 1097 | 526 | 52.0 | 899 | 1265 | 2164 |

[a] Uncertainty in observed shift values is ±200 $cm^{-1}$.
[b] In calculations, diameters (in Å unit) of an acetamide molecule, $Ca^{+2}$ and $NO_3^-$ ions are taken respectively as 4.52 Å [15], 2.0 [45] and 3.92 [46].

**Table 2**
Solvation timescales in molten mixtures of ($CH_3CONH_2$ + $Ca(NO_3)_2{\cdot}4.37H_2O$): comparison between experiments and different limits of the theory.

| $x_{salt}$ | Experiment[a] | | | | | Theory[b] | |
|---|---|---|---|---|---|---|---|
| | $\tau_1$ (ps) | $\tau_2$ (ps) | $a_1$ | $a_2$ | $\langle\tau_s\rangle$ (ps) | $\langle\tau_s\rangle_{ud}$ (ps) | $\langle\tau_s\rangle_{od}$ (ps) |
| 0.1 | 42 | 286 | 0.75 | 0.25 | 102 | 205 | 246 |
| 0.25 | 87 | 303 | 0.26 | 0.74 | 247 | 204 | 276 |
| 0.4 | 100 | 358 | 0.35 | 0.65 | 268 | 152 | 262 |
| 0.5 | 46 | 417 | 0.57 | 0.43 | 205 | 149 | 268 |

[a] Uncertainty in measured time constants are within ±5% of the reported values.
[b] While calculating $\langle\tau_s\rangle_x$ ($x$ = 'ud' or 'od') the total solvation response function is obtained as follows: $S(t) = 0.8S_{sd} + 0.2S_{si}$. Ref. [35] has shown that 'ion dynamics' affects the longtime dynamics and contributes ~20–25% to the total response function. 'ud' represents calculations done in the underdamped limit and 'od' those in the overdamped limit.

mentally measured frequency dependent dielectric function, $\varepsilon(\omega)$. In the absence of any reliable $\varepsilon(\omega)$ for these molten mixtures, we have approximated the dielectric relaxation time constants as those measured for liquid FA [39] but scaled by the viscosities of these molten mixtures, keeping the infinite frequency dielectric constant ($\varepsilon_\infty$) as that for FA. Use of acetamide dipole moment (3.7 D) in a statistical mechanical relation [40] leads to $\varepsilon_0 \approx 30$. In addition, a librational mode centered at 100 $cm^{-1}$ is included for the dispersion from $\varepsilon_0 \approx 5$ to $n_D^2 = 2.05$ ($n_D$ being the refractive index of acetamide). This is important as the high frequency response of the system is naturally contained in the timescale associated with the dispersion, $\varepsilon_\infty - n_D^2$. This calculation generates tri-exponential solvation response functions with time constants in the sub-hundred femtosecond (~30%), hundred picoseconds (~30–50%), and a few hundreds of picoseconds to nanosecond ranges (~20–40%). Interestingly, calculations in the overdamped limit, where frictional response is obtained only from diffusions using the stick hydrodynamic boundary condition, have also produced tri-exponential decay with the fastest time constant in the range of a few tens of picoseconds. The other two time constants are similar to those obtained in the underdamped limit. This indicates that the origin of the shorter timescale ($\tau_1$) detected in experiments and shown in Table 2 lies also in diffusion of medium particles, and the missing component arises largely from the participation of the collective intermolecular librational modes of acetamide molecules. One should also consider that rearrangement of water molecules, though present in a tiny proportion, can contribute to the missing portion of the dynamics [41,34]. More strikingly, none of these calculations indicate presence of solvation timescales any longer than approximately a nanosecond which is in sharp contrast to the continuum model prediction from the available dielectric relaxation data. Also, note that the calculated average solvation times in these two limits, $\langle\tau_s\rangle_{ud}$ and $\langle\tau_s\rangle_{od}$ are in semi-quantitative agreement with the corresponding experimental results.

We next investigate what are the relevant wavenumber modes density fluctuations at which generate the timescales observed in the present dynamic Stokes' shift measurements. It is to be noted that the timescales predicted by the present theory [15] is originating mainly from the relaxations of the orientational dipolar dynamic structure factor (ODSF) and the translational ion dynamic structure factor (TIDSF). In the diffusive limit, Eqs. (5) and (19) of the Appendix in Ref. [15] describe respectively the ODSF and TIDSF. Figure 5 shows the timescales originating from the diffusive relaxations associated with the nearest neighbor ($k\sigma \sim 2\pi$) and collective ($k\sigma \sim 0$) wavenumber modes of these dynamic structure factors. The data in this figure suggest that the experimentally observed shorter timescale originates from the orientational density

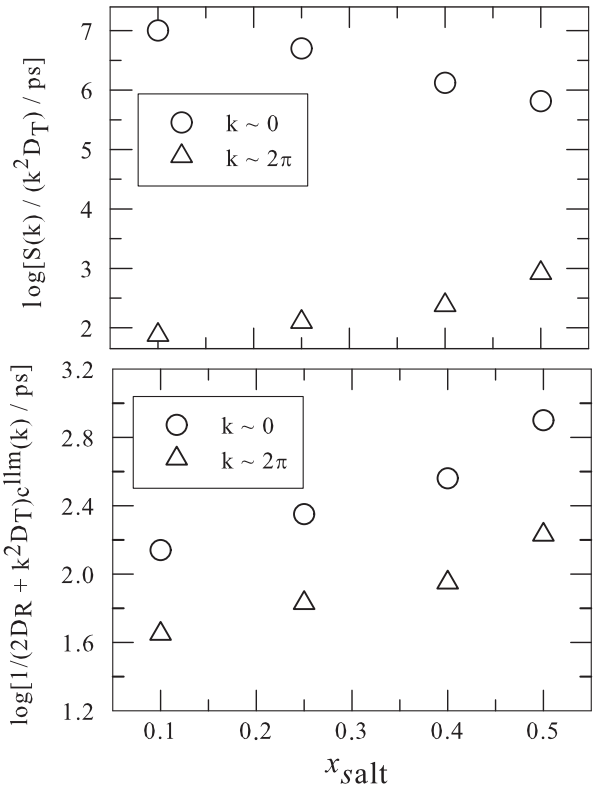


**Figure 5.** Length-scales of density fluctuations associated with the observed timescales in experiments: Relaxation time constants calculated in the overdamped limit for the translational ion dynamic structure factor (*upper panel*) and orientational dipolar dynamic structure factor (*lower panel*) are shown for $k\sigma \sim 0$ modes (circles) and $k\sigma \sim 2\pi$ modes (triangles) at ~318 K as a function of salt concentration. Note that orientational dipolar dynamic structure factor (ODSF) describes the timescale for angular readjustment of the dipolar solvent particles whereas the translational ion dynamic structure factor is associated with timescale arising from rearrangement via the centre-of-mass motion of the ions. For further details, see text.

fluctuations at $k\sigma \sim 2\pi$ modes whereas the longer timescale derive contributions from both the ion density fluctuations at $k\sigma \sim 2\pi$ and orientational density fluctuations at $k\sigma \sim 0$ modes. The collective ($k\sigma \sim 0$) ion density fluctuations generates an extremely slow timescale which has not been measured in the present experiments, indicating either the collective ion density fluctuations are irrelevant in Stokes' shift dynamics in these melts or the contribution is too small to be detected by the present experimental set-up.

The solute–medium interaction is further investigated by studying the fluorescence anisotropy of C153 in these molten mixtures at ~318 K. The biphasic time-resolved anisotropic decays in these melt mixtures have one time constant ranging between ~10 ps and ~30 ps, and the other between ~1 ns and ~4 ns. Measured average rotational times ($\langle\tau_{rot}\rangle$) and the corresponding slip and stick predictions (see Appendix 2) for a non-spherical solute [42] are shown in Figure 6 as a function of temperature-scaled viscosity ($\eta/T$) for these molten mixtures. It is evident from this figure that $\langle\tau_{rot}\rangle$ falls between the slip and stick predictions. Eventhough rotation data shown in Figure 6 are limited and a proper fractional power law dependence on $\eta/T$ cannot be constructed, $\langle\tau_{rot}\rangle$ in these melts are similar to those in molten mixtures of acetamide with $Na^+/K^+$ thiocyanates at comparable $\eta/T$ values [15]. This indicates that solute–medium interaction remains qualitatively similar in molten mixtures of (acetamide + electrolyte) even if $Ca^{+2}$ replaces $Na^+$ ions.

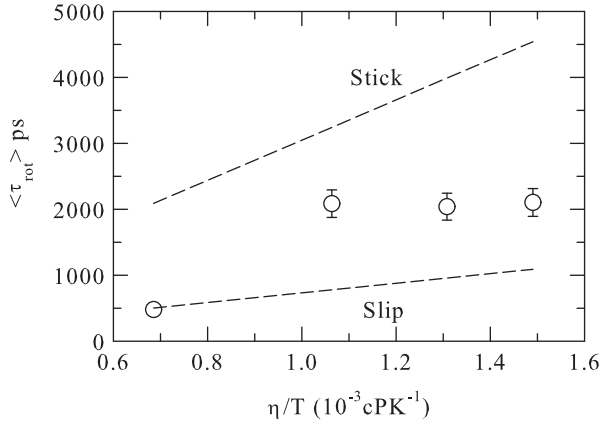


**Figure 6.** Coupling of solute rotation to the medium viscosity. Experimentally measured average rotation times at ~318 K are shown as a function of $x_{salt}$ ($r_0 = 0.38$). Predictions from the stick and the slip hydrodynamics for rotation of C153 (assuming ellipsoidal) are also shown. Error associated with the experimental data is typically ±10% of the reported values.

## 4. Conclusion

In summary, the present study reveals that $\varepsilon_0$ values of molten ($CH_3CONH_2 + Ca(NO_3)_2{\cdot}4.37H_2O$) mixtures are close to that of liquid formamide near room temperature and rearrangement of solvent particles in the immediate vicinity of the solute largely govern the solvation timescales detected in the present time-resolved experiments. The inability to fit the collected intensity decays to stretched exponentials suggest either much weaker heterogeneity than revealed by DR and other experiments, or, an effective 'averaging out' of the distinct solvent configurations due to relatively larger lifetime of the probe. In addition, time-resolved experiments do not exhibit any signatures of the reported mega-value of $\varepsilon_0$ and extremely slow relaxation time observed in DR experiments in the low frequency regime. The semi-molecular theory suggests substantial sub-picosecond response in these mixtures. This prediction and the heterogeneity aspects [43,44] should be explored in future studies.

## Acknowledgement

BG and SD are grateful to the CSIR, India for research fellowships.

## Appendix A. Supplementary data

Supplementary data associated with this article can be found, in the online version, at doi:10.1016/j.cplett.2010.12.003.

## References

[1] O.F. Stafford, J. Am. Chem. Soc. 55 (1933) 3987.
[2] D.H. Kerridge, Chem. Soc. Rev. 17 (1988) 181.
[3] G.E. McManis, A.N. Fletcher, D.E. Bliss, M.H. Miles, J. Electroanal. Chem. 190 (1985) 171.
[4] R.A. Wallace, Inorg. Chem. 11 (1972) 414.
[5] G. Berchiesi, G. Vitali, R. Plowiec, S. Barocci, J. Chem. Soc. Faraday Trans. 85 (1989) 635.
[6] J. Tripkovic, R. Nikolic, D.H. Kerridge, J. Serb. Chem. Soc. 54 (1989) 527.
[7] G. Berchiesi, F. Farhat, M.D. Angelis, J. Mol. Liq. 54 (1992) 103.
[8] R. Plowiec, A. Amico, G. Berchiesi, J. Chem. Soc. Faraday Trans. 2 (81) (1985) 217.
[9] S. Mahiuddin, J. Chem. Eng. Data 41 (1996) 231.
[10] G. Kalita, K.G. Sharma, S. Mahiuddin, J. Chem. Eng. Data 44 (1999) 222.
[11] M.L. Horng, J.A. Gardecki, A. Papazyan, M. Maroncelli, J. Phys. Chem. 99 (1995) 17311.
[12] R.S. Fee, J.A. Milsom, M. Maroncelli, J. Phys. Chem. 95 (1991) 5170.
[13] S. Arzhantsev, H. Jin, G.A. Baker, M. Maroncelli, J. Phys. Chem. B 111 (2007) 4978.
[14] H.K. Kashyap, R. Biswas, J. Phys. Chem. B 114 (2010) 254.
[15] B. Guchhait, H.A.R. Gazi, H.K. Kashyap, R. Biswas, J. Phys. Chem. B 114 (2010) 5066.
[16] B. Bagchi, R. Biswas, Adv. Chem. Phys. 109 (1999) 207.
[17] B. Bagchi, A. Chandra, Adv. Chem. Phys. 80 (1991) 1.
[18] B. Bagchi, Annu. Rev. Phys. Chem. 40 (1989) 115.
[19] P.G. Wolynes, J. Chem. Phys. 86 (1987) 5133.
[20] I. Rips, J. Klafter, J. Jortner, J. Chem. Phys. 88 (1988) 3246.
[21] J.E. Lewis, R. Biswas, A.G. Robinson, M. Maroncelli, J. Phys. Chem. B 105 (2001) 3306.
[22] W. Song, R. Biswas, M. Maroncelli, J. Phys. Chem. A 104 (2000) 6924.
[23] T. Pradhan, P. Ghoshal, R. Biswas, J. Phys. Chem. A 112 (2008) 915.
[24] T. Pradhan, P. Ghoshal, R. Biswas, J. Chem. Sci. 120 (2008) 275.
[25] Z. Hu, C.J. Margulis, Proc. Natl. Acad. Sci. USA 103 (2006) 831.
[26] P.K. Mandal, M. Sarkar, A. Samanta, J. Phys. Chem. A 108 (2004) 9048.
[27] F. Kremer, A. Schönhals, Broadband Dielectric Spectroscopy, Springer-Verlag, Heidelberg, 2003.
[28] G. Schroder, J. Hunger, A. Stoppa, R. Buchner, O. Steinhauser, J. Chem. Phys. 129 (2008) 184501.
[29] R.S. Fee, M. Maroncelli, Chem. Phys. 183 (1994) 235.
[30] C.F. Chapman, R.S. Fee, M. Maroncelli, J. Phys. Chem. 94 (1990) 4929.
[31] Y.J. Chang, E.W. Castner Jr., J. Phys. Chem. 98 (1994) 9712.
[32] Y.J. Chang, E.W. Castner Jr., J. Chem. Phys. 99 (1993) 113.
[33] H.K. Kashyap, R. Biswas, J. Chem. Phys. 125 (2006) 174506.
[34] N. Nandi, S. Roy, B. Bagchi, J. Chem. Phys. 102 (1995) 1390.
[35] R. Biswas, B. Bagchi, J. Phys. Chem. 100 (1996) 1238.
[36] C.F. Chapman, M. Maroncelli, J. Phys. Chem. 95 (1991) 9095.
[37] P. Eberspacher, E. Wismeth, R. Buchner, J. Barthel, J. Mol. Liq. 129 (2006) 3.
[38] T. Pradhan, R. Biswas, J. Phys. Chem. A 111 (2007) 11514.
[39] J. Barthel, R. Buchner, B. Wurm, J. Mol. Liq. 98–99 (2002) 51.
[40] C.G. Gray, K.E. Gubbins, Theory of Molecular Fluids, vol. 1, Clarendon, Oxford, UK, 1984.
[41] R. Jimenez, G.R. Fleming, P.V. Kumar, M. Maroncelli, Nature 369 (1994) 471.
[42] H. Jin, G.A. Baker, S. Arzhantsev, J. Dong, M. Maroncelli, J. Phys. Chem. B 111 (2007) 7291.
[43] S.E. Abraham, S.M. Bhattacharyya, B. Bagchi, Phys. Rev. Lett. 100 (2008) 167801.
[44] D. Chakrabarti, B. Bagchi, Phys. Rev. Lett. 96 (2006) 187801.
[45] R.D. Shanon, Acta Cryst. A 32 (1976) 751.
[46] W.L. Masterton, D. Bolocofsky, T.P. Lee, J. Phys. Chem. 75 (1971) 2809.